

Structuring of bridged silsesquioxanes *via* cooperative weak interactions: H-bonding of urea groups and hydrophobic interactions of long alkylene chains

Joël J. E. Moreau,* Benoît P. Pichon, Catherine Bied and Michel Wong Chi Man

Received 4th April 2005, Accepted 27th June 2005

First published as an Advance Article on the web 19th July 2005

DOI: 10.1039/b504635a

Lamellar-bridged silsesquioxanes were obtained by the acid-catalysed hydrolytic condensation of a series of bisilylated organobridged molecular precursors. It was found that exploiting cooperative effects between the molecular interactions created by long hydrophobic hydrocarbon chains and the H-bonding between urea groups in the precursors favoured the nanostructuring of the corresponding hybrid silicas.

Introduction

The sol-gel hydrolysis¹ of bis-trialkoxysilyl organics²⁻⁴ represents a fascinating bottom-up approach to hybrid organic-inorganic materials for targeted applications exploiting the properties of the incorporated organic fragments.⁵ During the past decade much effort has been directed towards producing organised and self-assembled hybrids^{2,3,6} and in the past five years, significant progress has been made using two synthetic strategies. On the one hand, periodic mesoporous bridged silsesquioxanes have been synthesized by the surfactant templating route as bulk materials⁷⁻¹⁰ and also as thin films and particulates.¹¹ On the other hand, the intrinsic self-assembly of the bridging organic units allowed the preparation of various self-organised hybrids.¹²⁻¹⁶ Our recent work involved the synthesis of bistrialkoxysilyl organics in which the organic units consist of a main organic substructure (chiral diaminocyclohexyl units, alkylene chains or phenyl ring) bridging two urea groups linked through a propylene chain (linker) to the silicon atoms on both sides.^{12,13} The controlled hydrolysis of these precursors led to hybrids structured on multiple length scales ranging from the nano- to the macro-scale range. Nevertheless, regardless of the method used, approaches for organising such hybrids are limited to the use of small organic units and the introduction of larger and more complex organic fragments remains a significant challenge.

In our recent work, in addition to identifying the key role of the H bonds between the urea groups in directing the assembly of the molecules into well defined supramolecular architectures, we also demonstrated the important role of the main organic substructure in defining the nanostructure¹² and the overall shapes of the resulting hybrid solids. However, significant difficulties in maintaining such ordered structures are encountered for even slight modification of the main organic substructure. The propylene linker connecting the urea

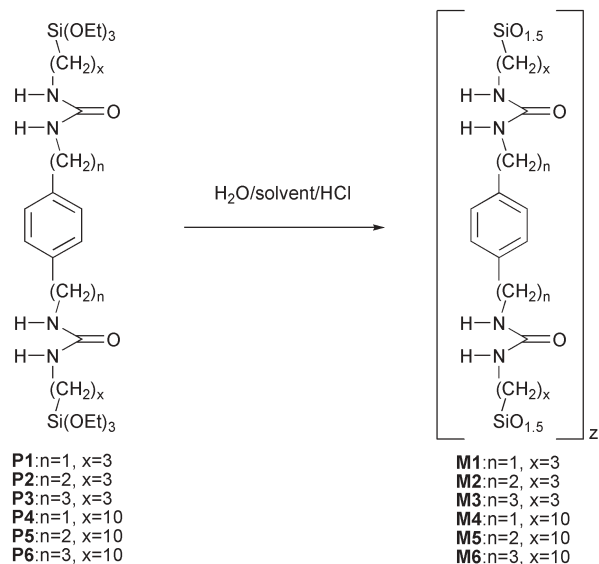
groups to the silicon atoms did not seem to affect the ordering imposed by the main organic group. However, replacing the propylene linker with longer alkylene bridges affected the basic properties of the molecular precursor, resulting in the facile formation of organogels.¹⁷ Furthermore, in the case of the chiral diaminocyclohexyl fragment as the main organic substructure, it was shown that the molecular interactions induced by C10 alkylene linkers play a more important structure-directing role than the intrinsic chirality of the main organic substructure for a C3 linker, modifying the helical fibers observed in the latter case to a lamellar form for the former.¹⁸ Considering these observations, we focused our work on the role of the alkylene linker and its contribution to controlling the structural evolution of the hybrids. Recently, we reported a crystalline hybrid $[\text{O}_{1.5}\text{Si}(\text{CH}_2)_3\text{NHCONH-Ph-NHCONH}(\text{CH}_2)_3\text{SiO}_{1.5}]_n$ with a rigid phenylene group directly connected to the two urea groups, with C3 alkylene linkers between the urea and the silicon atoms.¹² The nanoscale ordering of the organic molecules in the silica network were attributed to the H-bonding interaction of the urea group, possibly combined with the π -stacking of the rigid phenylene group. Here we describe the syntheses of a series of silylated phenylene compounds with C3 and C10 linkers and the corresponding hybrids obtained *via* sol-gel chemistry. In this work we investigated: (1) the influence of an additional flexible linker between the rigid bridging phenylene ring and the urea groups, changing from $-\text{Ph}-$ ¹² to $-(\text{CH}_2)_n-\text{Ph}-(\text{CH}_2)_n-$ (where n varies from 1 to 3; see Scheme 1) and; (2) the influence of the alkylene linker (C3 and C10 linkers) between the urea groups and the silicon atoms (see Scheme 1).

Experimental

Chemicals

1,4-Dibromobenzene, tris(*o*-tolylphosphine) (TOP), palladium acetate, palladium activated on carbon, 1 M borane solution in THF, (3-isocyanatopropyl)triethoxysilane and acrylonitrile were purchased from Aldrich, while 1,4-di(cyanomethyl)benzene and anhydrous sodium acetate were obtained from

Laboratoire Hétérochimie Moléculaire et Macromoléculaire (UMR-CNRS 5076), Ecole Nationale Supérieure de Chimie de Montpellier, 8 rue de l'école normale 34296 Montpellier Cedex 5, France. E-mail: joël.moreau@enscm.fr



Scheme 1 Syntheses of molecular precursors **P1–P6** and of the hybrid materials **M1–M6**.

Alfa Aesar. Dichloromethane was distilled over CaH_2 , while pentane and dimethylformamide were distilled over LiAlH_4 . Tetrahydrofuran was refluxed and distilled over LiAlH_4 and then further purified by distillation over sodium/benzophenone. (10-Isocyanatodecyl)triethoxysilane was synthesized in the laboratory.¹⁸ The molecular precursors were synthesized in Schlenk tubes under a nitrogen atmosphere.

Techniques

Melting points determinations were performed on an Electrothermal IA9000 Series apparatus. Elemental analyses were performed by the *Service Central de Microanalyse du CNRS* at Lyon–Vernaison. Mass spectra were measured on a JEOL JMS-DX 300 mass spectrometer. FT-IR spectra were recorded from KBr pellets using a PERKIN ELMER 1000. ^1H , ^{13}C and ^{29}Si liquid NMR spectra were recorded on a Bruker AC-200 or AC-250, with deuterated chloroform and dimethylsulfoxide used as solvents. Chemical shifts, δ , were indexed in ppm with respect to tetramethylsilane. ^{13}C and ^{29}Si CP-MAS solid state NMR spectra were recorded on a Bruker FT AM 400. Specific surface areas were measured by nitrogen adsorption–desorption and by BET analysis with a Micrometecs Gemini 2375 apparatus. Scanning electron microscopy (SEM) images were obtained from a JEOL 6300F microscope. Transmission electron microscopy (TEM) studies were performed on a JEOL 1200EX II. X-ray diffraction measurements and data treatment were performed at the *Groupe de Dynamique des Phases Condensées* in Montpellier. The X-ray diffraction experiments were carried out on solid powders in glass capillaries (1 mm diameter) in a transmission configuration. A copper rotating anode X-ray source (4 kW) with a multilayer focusing “Osmic” monochromator giving high flux (10^8 photons s^{-1}) and pinhole collimation was employed. An “image plate” 2D detector was used, and the data obtained were radially averaged to yield the diffracted intensity as a function of the wave vector, q .

The diffracted intensity was corrected for exposition time, transmission and the background scattering arising from an empty capillary.

Syntheses of molecular precursors

1,4-Di(aminoethyl)benzene^{19,20} (2). A solution of 780 mg (5 mmol) 1,4-di(cyanomethyl)benzene in 40 mL THF was introduced into a 3-necked round bottom flask under a nitrogen atmosphere. A 1 M borane solution in THF (35 mL) was added dropwise and the reacting mixture was refluxed for 24 h. The heating bath was removed and the solution was allowed to cool down to room temperature. The flask was placed in an ice bath and 40 mL of a 1 : 1 (v : v) mixture of THF– H_2O was carefully added dropwise, leading to a white precipitate. THF was removed *in vacuo* and then EtOH (80 mL) and concentrated H_2SO_4 (0.5 mL) were added. The mixture was heated under reflux for 30 min. The solvents were removed *in vacuo* and a 1 M NaOH solution was added to neutralize the acid. The amino compound was extracted with CHCl_3 . After drying over Na_2SO_4 , the solvents were removed leading to a white solid. Yield: 84% (686 mg, 4.18 mmol); mp: 60 °C; IR (CHCl_3 , cm^{-1}): 3358 (ν_{NH}); ^1H NMR (200 MHz, CDCl_3): δ = 1.08 (m, 4H, NH_2), 2.69 (t, 4H, CH_2), 2.92 (t, 4H, NCH_2), 7.11 (s, 4H, H_{ar}); ^{13}C NMR (50 MHz, CDCl_3): δ = 39.7 (CH_2), 43.6 (CH_2N), 128.9 (CH_{ar}) and 137.6 (C_{ar}); Mass (FAB): m/z (%): 165 (100) [$\text{M}+\text{H}$] $^+$.

1,4-Di(aminopropyl)benzene²¹ (3). The same procedure as above was used with 901 mg (4.90 mmol) of 1,4-di(cyanomethyl)benzene. Yield: 96% (900 mg, 4.69 mmol); mp: 72 °C; ^1H NMR (200 MHz, CDCl_3): δ = 1.22 (m, 4H, NH_2), 1.72 (qt, 4H, CH_2), 2.60 (t, 4H, ArCH_2), 2.69 (t, 4H, NCH_2), 7.07 (s, 4H, H_{ar}); ^{13}C NMR (50 MHz, CDCl_3): δ = 32.8 (CH_2), 35.4 (CH_2Ar), 41.8 (CH_2N), 128.3 (CH_{ar}) and 139.4 (C_{ar}); Mass (FAB): m/z (%): 192 (100).

1,4-Di(cyanovinyl)benzene (5). In a dry tube, 11.8 g (50 mmol) of 1,4-dibromobenzene and 8.2 g (100 mmol) of anhydrous sodium acetate were dissolved in 40 mL of anhydrous DMF. After 5 min stirring, 224.4 mg (1 mmol) of palladium acetate, 1.216 g (4 mmol) of *o*-tolylphosphine and 14.5 mL (0.22 mmol) of acrylonitrile were added. The mixture was frozen with liquid nitrogen and the tube was sealed. The reaction mixture was heated at 150 °C for 20 h. The catalyst was then removed by filtration at room temperature and washed with dichloromethane. The resulting filtrate was extracted with water. The organic phase was then dried over Na_2SO_4 and the solvent was removed *in vacuo*. A yellow solid was obtained after recrystallisation in a solution of acetonitrile–water. The three isomers (*trans-trans*, *cis-cis* and *cis-trans*) were obtained. Yield: 84% (7.55 g, 4.19 mmol); mp: 255 °C; IR (CHCl_3 , cm^{-1}): 2211 (ν_{CN}); ^1H NMR (200 MHz, CDCl_3): δ = 5.54 (d, 2H, CH_2 *cis*), 5.95 (d, 2H, CH_2 *trans*), 7.18 (dd, 2H, CH_2 *cis*), 7.35 (dd, 2H, CH_2 *trans*), 7.56 (d, 4H, CH_{ar} *cis-cis*), 7.81 (d, 4H, CH_{ar} *trans-trans*); ^{13}C NMR (50 MHz, CDCl_3): δ = 96.9 (CH_2 *cis*), 98.2 (CH_2 *trans*), 117.0 (CN_{cis}), 117.7 (CN_{trans}), 128.0 (CH_{ar} *cis*), 129.6 (CH_{ar} *trans*), 136.0 (CH_{ar} *cis-trans*), 147.2 (CH_2 *cis*), 149.1 (CH_2 *trans*); Mass (FAB): m/z (%): 180 (86);

Calculated elemental analysis for $C_{12}H_8N_2$ (%): C 79.97, H 4.48, N 15.55, found: C 79.97, H 4.41, N 15.42.

1,4-Di(cyanoethyl)benzene²² (6). 500 mg of Pd/C was added to a solution of 1g (5.55 mmol) of 1,4-di(cyanovinyl)benzene **5** dissolved in 40 mL of ethanol in a beaker. The solution was placed in an autoclave under hydrogen (5 bar) for 30 min. The mixture was filtered and the solvent was removed *in vacuo*. The remaining solid was dissolved in dichloromethane and extracted with a 1 M HCl solution. The organic phase was dried over Na_2SO_4 . The solvent was removed and the resulting powder was crystallised in an acetonitrile–water mixture to give white crystals. Yield: 93% (950 mg, 5.16 mmol); mp: 87 °C; IR ($CHCl_3$, cm^{-1}): 2243 (ν_{CN}); 1H NMR (200 MHz, $CDCl_3$): δ = 2.62 (t, 4H, CH_2), 2.95 (t, 4H, CH_2), 7.21 (s, 4H, CH_2); ^{13}C NMR (50 MHz, $CDCl_3$): δ = 19.2 (CH_2), 31.1 (CH_2), 119.2 (CN), 128.9 (CH_{ar}), 137.1 (C_{ar}); Mass (FAB): m/z (%): 184 (36).

1,4-Bis[(triethoxysilyl)propylureidomethyl]benzene (P1). 680 mg (5 mmol) of 1,4-di(aminomethyl)benzene **1** was dissolved in 40 mL of CH_2Cl_2 in a Schlenk tube under a nitrogen atmosphere. 2.59 g (10.5 mmol) of (3-isocyanatopropyl)triethoxysilane was added dropwise with a syringe and the reacting mixture was stirred overnight. The solvent was removed under vacuum. The solid obtained was washed with dry pentane to remove the excess isocyanate and then dried under vacuum to give a white powder. Yield: 85% (2.65 g; 2.05 mmol); mp: 194 °C; IR (KBr, cm^{-1}): 1583 (δ_{NH}), 1627 (ν_{CO}), 3334 (ν_{NH}); 1H NMR (200 MHz, DMSO D_6): δ = 0.52 (t, 4H, CH_2Si), 1.15 (t, 18H, CH_3), 1.42 (qt, 4H, CH_2), 2.97 (qd, 4H, CH_2), 3.74 (qd, 12H, OCH_2), 4.15 (d, 4H, CH_2), 5.92 (t, 2H, NH), 6.21 (t, 2H, NH), 7.16 (s, 4H, H_{ar}); ^{13}C NMR (50 MHz, $CDCl_3$): δ = 7.7 (CH_2Si), 18.2 (CH_3), 23.8, 42.8 and 44.0 (CH_2), 58.2 (CH_2O), 128.5 (CH_{ar}) and 137.7 (C_{ar}), 159.1 (CO); ^{29}Si NMR (50 MHz, DMSO D_6): δ = -45.0; Mass (FAB): m/z (%): 585 (74) [M-EtO] $^+$; Calculated elemental analysis $C_{28}H_{54}N_4O_8Si_2$ (%): C 53.30, H 8.63, N 8.88, found : C 52.97, H 8.57, N 8.91.

1,4-Bis[(triethoxysilyl)propylureidoethyl]benzene (P2). The same procedure as for **P1** was used, with 890 mg of 1,4-di(aminoethyl)benzene (**2**) (5.43 mmol) and 2.82 g (11.4 mmol) of (3-isocyanatopropyl)triethoxysilane leading to a white powder. Yield: 71% (2.53 g ; 3.85 mmol); mp: 188 °C; IR (KBr, cm^{-1}): 1582 (δ_{NH}), 1626 (ν_{CO}), 3339 (ν_{NH}); 1H NMR (200 MHz, $CDCl_3$): δ = 0.60 (t, 4H, CH_2Si), 1.20 (t, 18H, CH_3), 1.55 (qt, 4H, CH_2), 2.71 (t, 4H, CH_2), 3.08 (qt, 4H, CH_2), 3.34 (qd, 4H, CH_2), 3.79 (qd 12H, OCH_2), 4.77 (t, 2H, NH), 4.95 (t, 2H, NH), 7.07 (s, 4H, H_{ar}); ^{13}C NMR (50 MHz, $CDCl_3$): δ = 7.7 (CH_2Si), 18.2 (CH_3), 23.7, 36.1, 41.6 and 42.8 (CH_2), 58.1 (CH_2O), 128.7 (CH_{ar}) and 137.2 (C_{ar}), 159 (CO); ^{29}Si NMR (50 MHz, DMSO D_6): δ = -45.0; Mass (FAB): m/z (%): 613 (100) [M-EtO] $^+$; Calculated elemental analysis for $C_{30}H_{58}N_4O_8Si_2$ (%): C 54.68, H 8.87, N 8.50, found: C 54.74, H 8.77, N 8.65.

1,4-Bis[(triethoxysilyl)propylureidopropyl]benzene (P3). The same procedure as for **P1** was used with 1.16 g (6.04 mmol) of 1,4-di(aminopropyl)benzene (**3**) and 3.28 g (13.3 mmol) of

(3-isocyanatopropyl)triethoxysilane leading to a pink powder. Yield: 80% (3.31 g ; 4.83 mmol); mp: 120–121 °C; IR (KBr, cm^{-1}): 1581 (δ_{NH}), 1625 (ν_{CO}), 3334 (ν_{NH}); 1H NMR (200 MHz, $CDCl_3$): δ = 0.61 (t, 4H, CH_2Si), 1.16 (t, 18H, CH_3), 1.62 (t, 4H, CH_2), 1.75 (t, 4H, CH_2), 3.13 (qt, 8H, CH_2), 3.79 (qd 12H, OCH_2), 4.79 (t, 2H, NH), 4.88 (t, 2H, NH), 7.03 (s, 4H, H_{ar}); ^{13}C NMR (50 MHz, $CDCl_3$): δ = 7.6 (CH_2Si), 18.3 (CH_3), 23.7, 31.9, 32.7, 39.8 and 42.8 (CH_2), 58.3 (CH_2O), 128.3 (CH_{ar}) and 139.0 (C_{ar}), 159.9 (CO); ^{29}Si NMR (50 MHz, DMSO D_6): δ = -45.0; Mass (FAB): m/z (%): 641 (15) [M-EtO] $^+$; Calculated elemental analysis for $C_{32}H_{62}N_4O_8Si_2$ (%): C 55.94, H 9.10, N 8.15, found: C 55.73, H 9.13, N 8.28.

1,4-Bis[(triethoxysilyl)decylureidomethyl]benzene (P4). The same procedure as for **P1** was used with 560 mg (4.12 mmol) of 1,4-di(aminomethyl)benzene and 2.98 g (8.65 mmol) of (10-isocyanatodecyl)triethoxysilane leading to a white solid. Yield: 75% (2.55 g ; 3.09 mmol); mp: 189–191 °C; IR (KBr, cm^{-1}): 1579 (δ_{NH}), 1619 (ν_{CO}), 3345 (ν_{NH}); 1H NMR (200 MHz, $CDCl_3$): δ = 0.61 (t, 4H, CH_2Si), 1.21 (t, 18H, CH_3), 1.23–1.4 (m, 32H, CH_2), 3.16 (m, 4H, CH_2), 3.04 (m, 4H, CH_2), 3.72 (qd 12H, OCH_2), 5.97 (t, 2H, NH), 7.20 (s, 4H, H_{ar}), 8.13 (s, 2H, NH); ^{13}C NMR (50 MHz, DMSO): δ = 10.4 (CH_2Si), 18.3 (CH_3), 22.8, 27.3, 29.3, 29.4, 29.6, 30.6, 33.2 and 40.3 (CH_2), 40 (CH_2N), 58.3 (CH_2O), 129.0 (CH_{ar}) and 137.5 (C_{ar}), 159.2 (CO); ^{29}Si NMR (50 MHz, DMSO D_6): δ = -45.0; Mass (FAB): m/z (%): 826 (5); Calculated elemental analysis for $C_{42}H_{82}N_4O_8Si_2$ (%): C 60.98, H 10.00, N 6.78, found : C 61.02, H 9.96, N 7.07.

1,4-Bis[(triethoxysilyl)decylureidoethyl]benzene (P5). The same procedure as for **P1** was used with 387 mg (2.36 mmol) of 1,4-di(aminoethyl)benzene and 1.97 g (5.70 mmol) of (10-isocyanatodecyl)triethoxysilane giving a grey solid. Yield: 87% (1.75 g ; 2.05 mmol); mp: 156–158 °C; IR (KBr, cm^{-1}): 1578 (δ_{NH}), 1619 (ν_{CO}), 3346 (ν_{NH}); 1H NMR (200 MHz, DMSO D_6): δ = 0.54 (t, 4H, CH_2Si), 1.17 (t, 18H, CH_3), 1.23–1.4 (m, 32H, CH_2), 2.62 (t, 4H, CH_2), 2.40 (qd, 4H, CH_2), 3.22 (qd, 4H, CH_2), 3.73 (qd 12H, OCH_2), 5.72 (t, 2H, NH), 5.81 (t, 2H, NH), 7.10 (s, 4H, H_{ar}); ^{13}C NMR (50 MHz, DMSO D_6): δ = 9.8 (CH_2Si), 18.1 (CH_3), 23.4, 27.5, 31.6, 33.6, 33.8, 34.0, 34.2, 34.4, 35.2 and 37.5 (CH_2), 41.0 (CH_2N), 58.8 (CH_2O), 129.8 (CH_{ar}) and 138.6 (C_{ar}), 159.1 (CO); ^{29}Si NMR (50 MHz, DMSO D_6): δ = -45.0; Mass (FAB): m/z (%): 854 (6); Elemental analysis for $C_{44}H_{86}N_4O_8Si_2$ (%): C 61.78, H 10.13, N 6.55, found: C 61.55, H 10.09, N 6.87.

1,4-Bis[(triethoxysilyl)decylureidopropyl]benzene (P6). The same procedure as for **P1** was used with 300 mg (1.63 mmol) of 1,4-di(aminopropyl)benzene and 1.34 g (3.90 mmol) of (10-isocyanatodecyl)triethoxysilane leading to a pink solid. Yield: 76% (1.09 g ; 1.24 mmol); mp: 113–115 °C; IR (KBr, cm^{-1}): 1578 (δ_{NH}), 1623 (ν_{CO}), 3337 (ν_{NH}); 1H NMR (200 MHz, DMSO D_6): δ = 0.54 (t, 4H, CH_2Si), 1.13 (t, 18H, CH_3), 1.23 to 1.4 (m, 40H, CH_2), 3.00 (m, 8H, CH_2), 3.72 (qd 12H, OCH_2), 5.74 (t, 2H, NH), 5.80 (t, 2H, NH), 7.08 (s, 4H, H_{ar}); ^{13}C NMR (50 MHz, DMSO D_6): δ = 9.8 (CH_2Si), 18.1 (CH_3), 22.2, 26.3, 28.5, 28.7, 28.8, 28.9, 29.9, 31.8, 32.0, 32.2 and 41.5 (CH_2), 57.5 (CH_2O), 138.9 (CH_{ar}) and 157.0

(C_{ar}), 158.4 (CO); ^{29}Si NMR (50 MHz, DMSO d_6): -44.9 ; Mass (FAB): m/z (%): 883 (23) $[\text{M}+\text{H}]^+$; Calculated elemental analysis for $\text{C}_{46}\text{H}_{90}\text{N}_4\text{O}_8\text{Si}_2$ (%): C 62.54, H 10.27, N 6.34, found: C 62.28, H 10.15, N 6.75.

Syntheses of the hybrid materials

Hybrid silica M1. 125 mg (0.20 mmol) of 1,4-bis[(triethoxysilyl)propylureidomethyl]benzene **P1** was dissolved in 2 mL of ethanol. Then 2.2 mL of distilled water were added while stirring. A white precipitate appeared. 33.4 μL of a 1 M HCl solution was added. The following molar ratio was used: precursor: 1, EtOH: 170, H_2O : 600, HCl: 0.2. After heating the reaction mixture at 60 $^\circ\text{C}$ the precipitate completely dissolved in a few minutes. After 2 h a precipitate appeared and the mixture was aged under static conditions. After 4.5 days, the solvents were removed by filtration. The solid product was washed successively with water, ethanol, acetone and finally dried at 110 $^\circ\text{C}$. A grey powder was obtained. IR (KBr, cm^{-1}): 1560 (δ_{NH}), 1654 (ν_{CO}) and 3370 (ν_{NH}); ^{13}C NMR CPMAS (ppm): 10.7, 25.2, 43.4 (2 C), 127.4, 139.5, 160.1; ^{29}Si NMR CPMAS (ppm): -57.8 , -65.7 (T^2 and T^3 sites); specific surface area: 8.9 $\text{m}^2 \text{g}^{-1}$. Found elemental analysis: C 44.25, H 6.23, N 12.86, Si 12.90.

Hybrid silica M2. The hybrid silica **M2** was obtained using the same conditions as **M1** with 132 mg (0.20 mmol) of 1,4-bis[(triethoxysilyl)propylureidoethyl]benzene **P2** leading to a white powder. IR (KBr, cm^{-1}): 1560 (δ_{NH}), 1638 (ν_{CO}) and 3423 (ν_{NH}); ^{13}C NMR CPMAS (ppm): 10.9, 24.6, 33.5, 41.5 (2 C), 129.7, 137.4, 160.1; ^{29}Si NMR CPMAS (ppm): -56.8 , -65.2 (T^2 and T^3 sites); Specific surface area: 6.1 $\text{m}^2 \text{g}^{-1}$.

Hybrid silica M3. Hybrid silica **M3** was obtained using the same conditions as **M1** with 138 mg (0.2 mmol) of 1,4-bis[(triethoxysilyl)propylureidopropyl]benzene **P7** to give a white powder. IR (KBr, cm^{-1}): 1570 (δ_{NH}), 1638 (ν_{CO}) and 3424 (ν_{NH}); ^{13}C NMR CPMAS (ppm): 11.6, 24.1, 32.4, 35.0, 41.3, 43.5, 128.6, 139.3, 160.1; ^{29}Si NMR CPMAS (ppm): -57.7 , -66.0 (T^2 and T^3 sites); Specific surface area: 14.3 $\text{m}^2 \text{g}^{-1}$.

Hybrid silica M4. 165 mg (0.2 mmol) of 1,4-bis[(triethoxysilyl)decylureidomethyl]benzene **P4** was dissolved in 2.6 mL of dimethylsulfoxide by heating. A gel was obtained when the solution was cooled down to room temperature. 1.6 mL of distilled water was added with stirring. A white precipitate formed, and then 33.4 μL 1 M HCl solution was added. The following molar ratios were used: precursor: 1, DMSO: 245, H_2O : 600, HCl: 0.2. The mixture was heated at 60 $^\circ\text{C}$ for 2 h and then the stirring was stopped. No solubilisation of the precipitate was observed during the whole reaction. After 4.5 days at 60 $^\circ\text{C}$, the solution was filtered and the solid was washed successively with water, ethanol and acetone and then dried overnight at 110 $^\circ\text{C}$ leading to a white powder. IR (KBr, cm^{-1}): 1583 (δ_{NH}), 1622 (ν_{CO}) and 3354 (ν_{NH}); ^{13}C NMR CPMAS (ppm): 13.6, 24.3, 32.0 (9 C), 40.1, 42.6, 128.9, 138.0, 159.3; ^{29}Si NMR CPMAS (ppm): -47.9 , -57.4 , -66.9 (T^1 , T^2 and T^3 sites); Specific surface area: 10.1 $\text{m}^2 \text{g}^{-1}$; Found elemental analysis (%): C 58.35, H 8.55, N 9.23, Si 8.90.

Hybrid silica M5. The hybrid silica **M5** was obtained in the same way as **M4**, with 168 mg (0.2 mmol) of 1,4-bis[(triethoxysilyl)decylureidoethyl]benzene (**P5**). A white powder was obtained. IR (KBr, cm^{-1}): 1578 (δ_{NH}), 1625 (ν_{CO}) and 3356 (ν_{NH}); ^{13}C NMR CPMAS (ppm): 14.7, 23.9, 31.6 (10 C), 42.3, 128.7, 136.5, 160.5; ^{29}Si NMR CPMAS (ppm): -48.5 , -57.1 , -67.5 (T^1 , T^2 and T^3 sites); Specific surface area: 10.2 $\text{m}^2 \text{g}^{-1}$. Found elemental analysis: C 58.56, H 8.26, N 8.75, Si 9.19.

Hybrid silica M6. The hybrid silica **M6** was obtained in the same way as **M4** with 176 mg (0.2 mmol) of 1,4-bis[(triethoxysilyl)decylureidopropyl]benzene (**P6**). A white powder was obtained. IR (KBr, cm^{-1}): 1580 (δ_{NH}), 1631 (ν_{CO}) and 3353 (ν_{NH}); ^{13}C NMR CPMAS (ppm): 13.5, 31.9 (22 C), 40.4, 128.1, 136.9, 159.3; ^{29}Si NMR CPMAS (ppm): -48.4 , -57.0 , -66.4 (T^1 , T^2 and T^3 sites); Specific surface area: 14.5 $\text{m}^2 \text{g}^{-1}$.

Results and discussion

Preparation of the molecular precursors and the hybrids

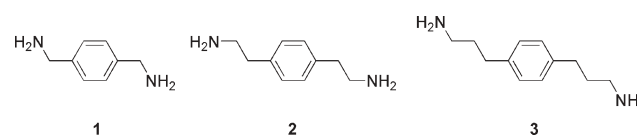
The molecular precursors and the corresponding hybrids obtained by their hydrolysis are given in Scheme 1.

P1–P6 were synthesised from three different diamines (Scheme 2). 1,4-(diaminomethyl)benzene, **1**, is commercially available and 1,4-(diaminoethyl)benzene (**2**) and 1,4-(diaminopropyl)benzene (**3**) were synthesised according to Scheme 3 and 4, respectively.

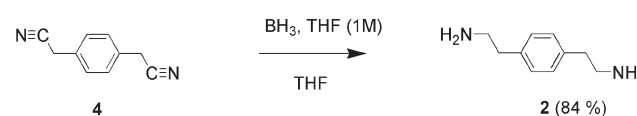
Diamine **2** was obtained in high yield (84%) from 1,4-di(cyanomethyl)benzene **4** by the reduction of the two nitrile groups with $\text{BH}_3 \cdot \text{THF}$ (Scheme 3).

Diamine **3** was synthesised in three steps (Scheme 4). 1,4-dibromobenzene was treated using Heck's reaction with acrylonitrile in the presence of tris(*o*-tolyl)phosphine (TOP) and $\text{Pd}(\text{OAc})_2$ as catalysts in DMF. In this case, a mixture of the three possible isomers **5** (*cis-cis*, *trans-trans* and *cis-trans*) was obtained. Treatment of this mixture with hydrogen gas (5 bar) in an autoclave with Pd/C as catalyst gave **6**. The latter was reduced with $\text{BH}_3 \cdot \text{THF}$ to give **3** in a good overall yield (75%).

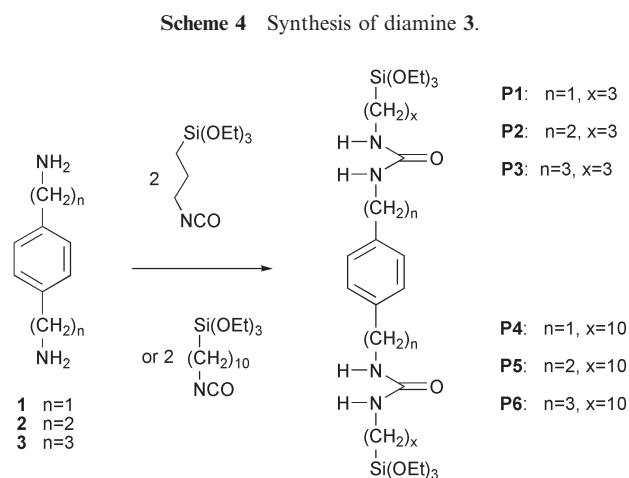
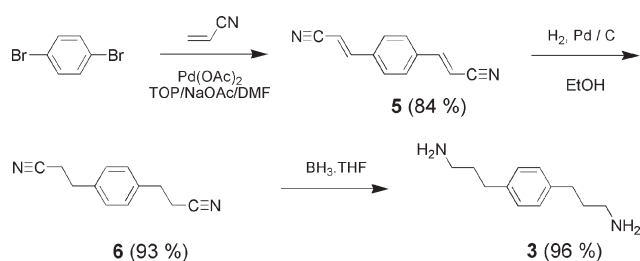
The reaction of 3-(isocyanatopropyl)triethoxysilane and 10-(isocyanatodecyl)triethoxysilane with the three diamines in CH_2Cl_2 yielded the six molecular precursors (Scheme 5).



Scheme 2 Starting diamines **1–3** for the synthesis of **P1–P6**.



Scheme 3 Synthesis of diamine **2**.



Scheme 5 Synthesis of precursors **P1–P6**.

Syntheses of the hybrids **M1–M6**

The hybrid materials with the shorter C3 linker ($x = 3$) **M1–M3** (see Scheme 1) were obtained by acid-catalysed hydrolysis in a mixture of water and ethanol with the following molar ratio: **P1–P3**: 1, EtOH: 170, H₂O: 600, HCl: 0.2. For those with longer linkers ($x = 10$, **M4–M6**) the reaction was performed in a mixture of water and DMSO due to the insolubility of the corresponding precursors **P4–P6** in ethanol. The molar ratio was **P4–P6**: 1, DMSO: 245, H₂O: 600, HCl: 0.2. The reactions were all conducted at 60 °C over 4.5 days. Solid materials were obtained after filtering the solutions, successive washings with water, ethanol and acetone followed by drying at 110 °C.

Characterisations of the hybrid materials **M1–M6**

We studied the composition of the hybrids by elemental analysis. Since all hybrids were synthesised under the same conditions apart from the solvents (ethanol for **M1–M3**) and DMSO for **M4–M6**), we examined only **M1** and **M4**. In both cases, a ratio Si/N of 0.48 was found, which is close to the theoretical value of 0.5 indicating that the organic fragments are quantitatively present in the solid materials.

We further studied these compositions by solid state NMR (¹³C and ²⁹Si). The solid state ¹³C CP-MAS NMR spectra (Figs. 1 and 2) exhibit several peaks characteristic of the organic fragments with chemical shifts at 160 (CO), 136 and 129 (aromatic ring) and from 11 to 42 ppm (CH₂). The signal at 11 ppm corresponds to the C–Si, confirming that cleavage of the C–Si bond did not occur during hydrolysis. The ¹³C CP-MAS NMR spectra of **M1** (Fig. 1) and **M4** (Fig. 2) are shown as examples.

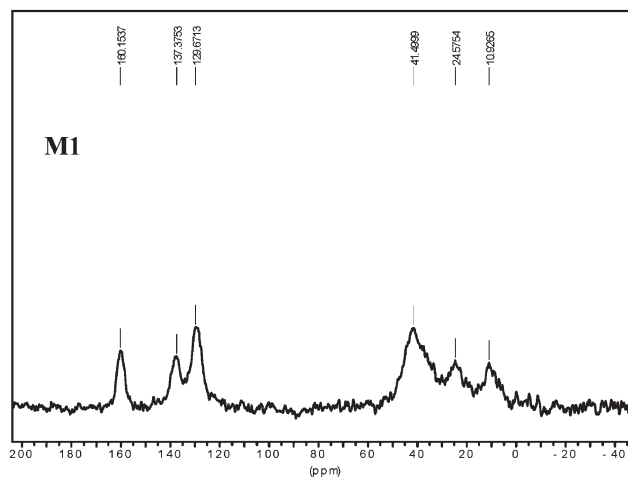


Fig. 1 Solid state ¹³C CP-MAS NMR of **M1**.

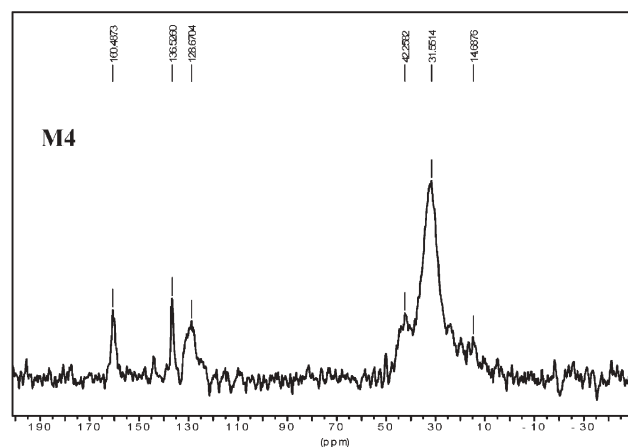


Fig. 2 Solid state ¹³C CP-MAS NMR of **M4**.

It can be seen that for the sample incorporating a long alkylene linker (**M4**), the peak at around 30 ppm is relatively intense, as expected, due to the greater number of carbon atoms from the C10 alkylene chain.

The complete conservation of the C–Si bonds was confirmed by ²⁹Si CP-MAS NMR studies. This is exemplified by the spectra of **M1** and **M4** (Fig. 3). In the case of the sample **M1**, which incorporates the shorter linker, both T² [C–Si(OSi)₂OR],

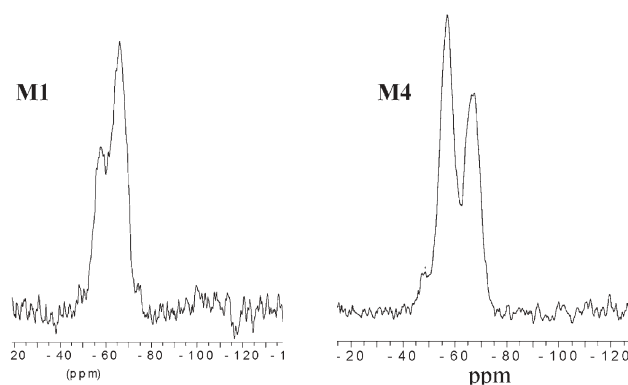


Fig. 3 Solid state ²⁹Si CP-MAS NMR of **M1** and **M4**.

minor peak] and T^3 units [$C-Si(OSi)_3$, major peak] are observed, reflecting a highly condensed material. The spectra of **M2** and **M3** are similar, with a degree of condensation of 90–94%.

The spectra of the samples incorporating the longer linker (**M4–M6**) are identical. As exemplified in Fig. 3 in the case of **M4**, these latter solids are less condensed (degree of condensation = 74–80%). Three peaks can be distinguished, corresponding to T^1 [$C-Si(OR)_2OSi$], T^2 [$C-Si(OSi)_2OR$] and T^3 [$C-Si(OSi)_3$] units, with the T^2 unit being predominant. The hydrophobic properties and the steric bulk of the long C10 alkylene linker may account for the decreasing rate of hydrolysis and condensation.

We also examined the H-bonding strength of the urea groups by FT-IR studies of the hybrids. This can be probed by monitoring the positions of the amide 1 ($\nu_{CO} \approx 1650\text{ cm}^{-1}$) and amide 2 modes ($\delta_{NH} \approx 1570\text{ cm}^{-1}$). The difference between these two vibrations ($\Delta\nu$) gives a good indication of the strength of the H-bonds between the urea groups,^{23–25} with a low $\Delta\nu$ value indicating strong H-bonding interactions. Interestingly, low $\Delta\nu$ values were obtained for **M4–M6** whereas those for the short linker hybrids **M1–M3** were larger (ranging from 68 to 94 cm^{-1}) which reflects stronger H-bonds in the former materials. Moreover, this effect is also evident from the amide A ($\nu_{NH} \approx 3400\text{ cm}^{-1}$) vibration, where a shift towards lower wavenumbers corresponds to stronger H-bonding between the urea groups.²³ The results are in good agreement with those of the $\Delta\nu$ values since the ν_{NH} values of **M4–M6** range from 3353 to 3356 cm^{-1} . In contrast, those for **M1–M3** are observed at higher wavenumbers (3370–3423 cm^{-1}). From these observations it can be seen that the organic fragments in the long linker materials are better assembled than in the short linker hybrids. The hydrophobic interactions of the long alkylene linkers influence the self-association of the molecules during the hydrolysis.

We then analysed the powder X-ray diffraction (PXRD) patterns of these materials. The two broad peaks at around 16 and 4.5 Å in the diffractograms of hybrids **M1–M3** signify that these materials are amorphous, although the narrower peaks in

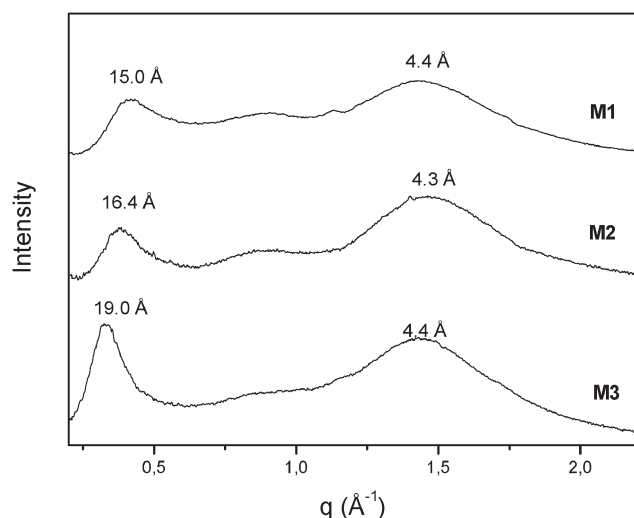


Fig. 4 PXRD of **M1–M3**.

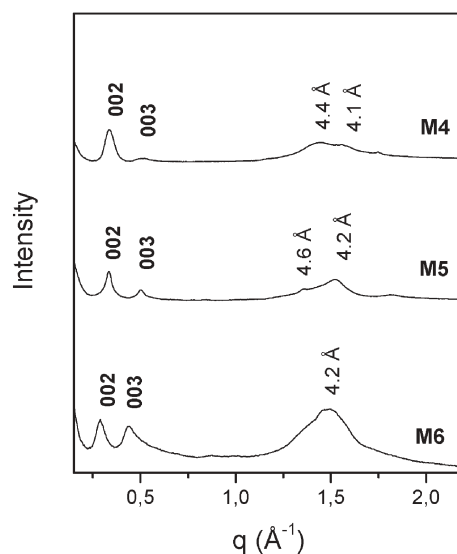


Fig. 5 PXRD of **M4–M6**.

the case of **M3** reflect a slightly better organisation in this hybrid compared with **M1** and **M2** (Fig. 4).

The PXRD of hybrids **M4–M6** are different (Fig. 5) with several well-resolved peaks being observed.

These materials are more organised than the short linker hybrids since their diffractograms exhibit sharper peaks, particularly at low q values (Fig. 6). Indeed, three peaks are observed. The very small peak at 36.9, 37.7 and 43.7 Å for **M4–M6**, respectively, can be attributed to a first-order harmonic (001) of lamellar structures since the other peaks in the three PXRD patterns are at repetitive intervals with respect to the first one and are assigned as the second (002) and the third (003) harmonics.

The first-order distances in the three hybrids are comparable to the length of the organic fragments. The hydrophobic interactions due to the long alkylene chains here compensate

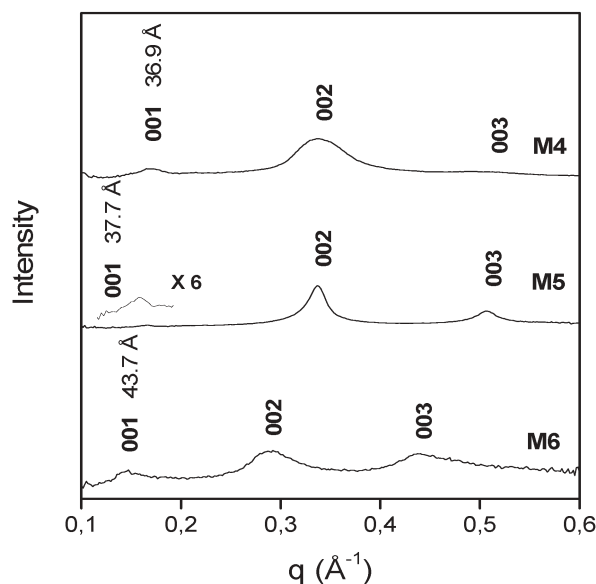


Fig. 6 PXRD of **M4–M6** at low angle.

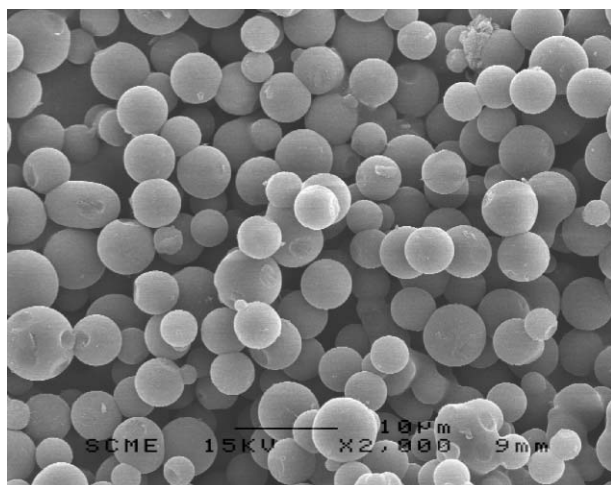


Fig. 7 SEM image of M1.

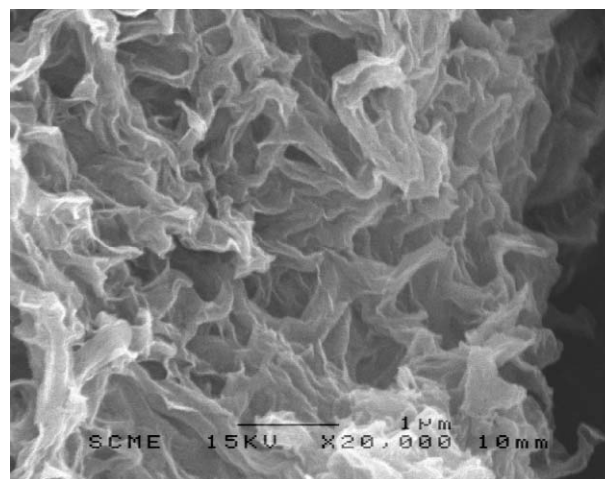


Fig. 9 SEM image of M4.

for the disorder created by the flexibility of the C1, C2 and C3 carbon chains between the phenylene ring and the urea groups.

Interesting features can be observed from electron microscopy analyses of M1–M3, which consist of spheres with diameters ranging from 1 to 8 μm as seen from the SEM (scanning electron microscopy) image of M1 (Fig. 7).

From the TEM (transmission electron microscopy) image, the sphere as represented for M1 is completely dark showing that the hybrid is a dense material, with little electron contrast (Fig. 8).

For these short linker materials, the hydrolysis of the precursors took place in a homogeneous way at the beginning, with the precursors dissolving in the solution on heating. This leads to a conventional nucleation and growth process which can explain the formation of spheres.

The hybrids M4–M6 are similar when observed by SEM and they resemble flexible films, as illustrated in Fig. 9 for M4.

The TEM image of M4 is presented as an example in Fig. 10, the hybrids M5 and M6 showing similar features. The results from the TEM pictures confirm the lamellar structures of hybrids M4–M6 and these results correlate with those of the

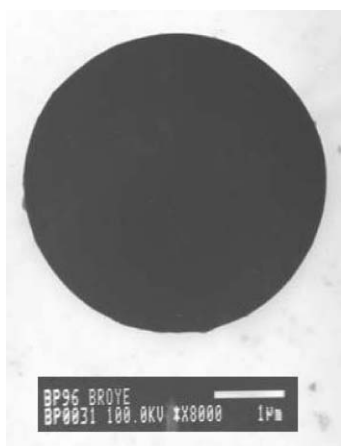


Fig. 8 TEM image of M1.

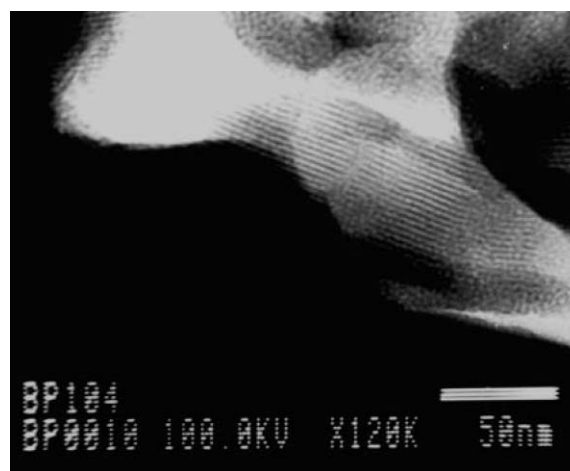


Fig. 10 TEM image of M4.

PXRD analyses. Well-aligned stripes with similar distances with those obtained from the PXRD are observed.

Conclusion

In this work, we describe the synthesis of new lamellar hybrid silsesquioxanes by combining two weak molecular interactions based on H-bonding and hydrophobic effects. The latter resulted from the incorporation of long alkylene chains and it is shown that such hydrophobic interactions can compensate for disordering effects arising from the presence of flexible alkylene chain (C1, C2 and C3) directly bonded to a rigid phenylene ring. This strategy provides a synthetic approach to the design of nanostructured, bridged silsesquioxanes and may offer the possibility of extending the nanostructuring of bridged silsesquioxanes to a wide range of organic functionalities.

Acknowledgements

This work was supported by the CNRS and the Ministère de la Recherche (ACI Nanosciences-Nanotechnologies).

References

- C. J. Brinker and G. W. Scherer, *Sol–Gel Science: the Physics and Chemistry of Sol–Gel Processing*, Academic Press, San Diego, 1990.
- K. J. Shea, D. A. Loy and O. W. Webster, *J. Am. Chem. Soc.*, 1992, **114**, 6700–6710; D. A. Loy and K. J. Shea, *Chem. Rev.*, 1995, **95**, 1431–1442; K. J. Shea and D. A. Loy, *Chem. Mater.*, 2001, **19**, 3306–3319.
- R. J. P. Corriu, J. J. E. Moreau, P. Thépot and M. Wong Chi Man, *Chem. Mater.*, 1992, **4**, 1217–1224; J. J. E. Moreau and M. Wong Chi Man, *Coord. Chem. Rev.*, 1998, **178–180**, 1073–1084; R. J. P. Corriu, *Angew. Chem., Int. Ed.*, 2000, **39**, 1376–1398.
- K. J. Shea, J. J. E. Moreau, D. A. Loy, R. J. P. Corriu and B. Boury, *Functional Hybrid Materials*, ed. P. Gomez-Romero and C. Sanchez, Wiley-VCH, 2004, p. 50 and references therein.
- Organic/Inorganic Hybrid Materials, MRS Symp.*, ed. R.M. Laine, C. Sanchez, C.J. Brinker and E. Giannelis, Materials Research Science, Warrendale, PA, 1998, vol. 519; *Organic/Inorganic Hybrid Materials III, MRS Symp.*, ed. R.M. Laine, C. Sanchez, C.J. Brinker and E. Giannelis, Materials Research Science, Warrendale, PA, 2000, vol. 628.
- B. Boury, R. J. P. Corriu, V. Le Strat, P. Delord and M. Nobili, *Angew. Chem., Int. Ed.*, 1999, **38**, 3172–3173; F. Ben, B. Boury, R. J. P. Corriu, P. Delord and M. Nobili, *Chem. Mater.*, 2002, **14**, 730–738.
- S. Guan, S. Inagaki, T. Ohsuna and O. Terasaki, *J. Am. Chem. Soc.*, 2000, **122**, 5660–5661; M. P. Kapoor, Q. Yang and S. Inagaki, *J. Am. Chem. Soc.*, 2002, **124**, 15176–15177; S. Inagaki, S. Guan, T. Ohsuna and O. Terasaki, *Nature*, 2002, **416**, 304–307.
- B. J. Melde, B. T. Holland, C. F. Blanford and A. Stein, *Chem. Mater.*, 1999, **11**, 3302–3308.
- T. Asefa, M. J. MacLachlan, M. Coombs and G. A. Ozin, *Nature*, 1999, **402**, 867–871; M. J. MacLachlan, T. Asefa and G. A. Ozin, *Chem.—Eur. J.*, 2000, **6**, 2507–2511.
- A. Sayari, S. Hamoudi, Y. Yang, I. L. Moudrakovski and J. R. Ripmeester, *Chem. Mater.*, 2000, **12**, 3857–3863.
- Y. Lu, H. Fan, N. Doke, D. A. Loy, R. A. Assink, D. LaVan and C. J. Brinker, *J. Am. Chem. Soc.*, 2000, **122**, 5258–5261.
- J. J. E. Moreau, L. Vellutini, M. Wong Chi Man, C. Bied, J.-L. Bantignies, P. Dieudonné and J.-L. Sauvajol, *J. Am. Chem. Soc.*, 2001, **123**, 7957–7958; J. J. E. Moreau, B. P. Pichon, M. Wong Chi Man, C. Bied, H. Pritzkow, J.-L. Bantignies, P. Dieudonné and J.-L. Sauvajol, *Angew. Chem., Int. Ed.*, 2004, **43**, 203–206; J. J. E. Moreau, L. Vellutini, M. Wong Chi Man, C. Bied, P. Dieudonné, J.-L. Bantignies and J.-L. Sauvajol, *Chem.—Eur. J.*, 2005, **11**, 1527–1537.
- J. J. E. Moreau, L. Vellutini, M. Wong Chi Man and C. Bied, *J. Am. Chem. Soc.*, 2001, **123**, 1509–1510; J. J. E. Moreau, L. Vellutini, M. Wong Chi Man and C. Bied, *Chem.—Eur. J.*, 2003, **9**, 1594–1999.
- N. Liu, K. Yu, B. Smarsly, D. R. Dunphy, Y.-B. Jiang and C. J. Brinker, *J. Am. Chem. Soc.*, 2002, **124**, 14540–14541.
- H. Muramatsu, B. Boury and R. J. P. Corriu, *J. Am. Chem. Soc.*, 2003, **125**, 854.
- Y. Yang, M. Nakazawa, M. Suzuki, M. Kimura, H. Shirai and K. Hanabusa, *Chem. Mater.*, 2004, **16**, 3791–3793.
- O. Dautel, J.-P. Lère-Porte, J. J. E. Moreau and M. Wong Chi Man, *Chem. Commun.*, 2003, 2662–2663.
- Xu Qinghong, J. J. E. Moreau and M. Wong Chi Man, *J. Sol–Gel Sci. Technol.*, 2004, **32**, 111–115.
- A. F. Titley, *J. Chem. Soc.*, 1926, **128**, 508–519.
- P. Ruggli and B. Prijs, *Helv. Chim. Acta*, 1945, **28**, 674–686.
- L. K. Freidlin, T. A. Sladkova, G. I. Kudryavtsev, T. I. Shein, E. N. Zil'berman and R. G. Federova, *Bull. Acad. Sci. USSR Div. Chem. Sci. (Engl. Transl.)*, 1961, **10**, 1598–1600.
- H. Paul and S. Tchelitchefft, *Bull. Soc. Chim. Fr.*, 1949, 470–475.
- J. Jadzyn, M. Stockhauser and B. Zywuicki, *J. Phys. Chem.*, 1987, **91**, 754–757.
- M. de Loos, J. van Esch, I. Stokroos, R. M. Kellogg and B. L. Feringa, *J. Am. Chem. Soc.*, 1997, **119**, 12675–12676; J. van Esch, F. Schoonbeek, M. de Loos, H. Kooijman, A. L. Spek, R. M. Kellogg and B. L. Feringa, *Chem.—Eur. J.*, 1999, **5**, 937–950; M. de Loos, J. van Esch, R. M. Kellogg and B. L. Feringa, *Angew. Chem., Int. Ed.*, 2001, **40**, 613–616; V. D. Laan, B. Feringa, R. M. Kellogg and J. van Esch, *Langmuir*, 2002, **18**, 7136–7140.
- F. Lortie, S. Boileau and L. Bouteiller, *Chem. Eur. J.*, 2003, **9**, 3008–3014; V. Simic, L. Bouteiller and M. Jalabert, *J. Am. Chem. Soc.*, 2003, **125**, 13148–13154.